

## Self-assembled Fe nanodots on Ge(001)

K. Jordan and I. V. Shvets

Citation: [Applied Physics Letters](#) **88**, 193111 (2006); doi: 10.1063/1.2201861

View online: <http://dx.doi.org/10.1063/1.2201861>

View Table of Contents: <http://scitation.aip.org/content/aip/journal/apl/88/19?ver=pdfcov>

Published by the [AIP Publishing](#)

---

### Articles you may be interested in

[Nonvolatile memories of Ge nanodots self-assembled by depositing ultrasmall amount Ge on Si O<sub>2</sub> at room temperature](#)

Appl. Phys. Lett. **92**, 093124 (2008); 10.1063/1.2892494

[Periodic arrays of epitaxial self-assembled SiGe quantum dot molecules grown on patterned Si substrates](#)

J. Appl. Phys. **100**, 084312 (2006); 10.1063/1.2358003

[Formation and evolution of self-assembled crystalline Si nanorings on \(001\) Si mediated by Au nanodots](#)

Appl. Phys. Lett. **87**, 223102 (2005); 10.1063/1.2136219

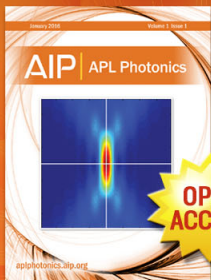
[Patterning of sub-10-nm Ge islands on Si\(100\) by directed self-assembly](#)

Appl. Phys. Lett. **87**, 171902 (2005); 10.1063/1.2112198

[Long-range ordered lines of self-assembled Ge islands on a flat Si \(001\) surface](#)

Appl. Phys. Lett. **77**, 4139 (2000); 10.1063/1.1326842

---



Launching in 2016!  
The future of applied photonics research is here

AIP | APL  
Photonics

## Self-assembled Fe nanodots on Ge(001)

K. Jordan<sup>a)</sup> and I. V. Shvets

SFI Laboratories, School of Physics, Trinity College, Dublin 2, Ireland

(Received 21 December 2005; accepted 20 March 2006; published online 9 May 2006)

The initial nucleation of Fe onto the  $(2 \times 1)$  reconstructed Ge(001) surface is studied. Uniformly sized two-dimensional Fe dots are shown to nucleate. They have an apparent corrugation height  $\sim 1.1 \text{ \AA}$  and lateral dimensions  $\sim 12 \times 8 \text{ \AA}^2$ . Further to their uniform size, due to their registry with respect to the substrate, they are shown to nucleate on a single equivalent surface site. It is suggested that their stability is due to either a “magic” number effect or adsorbate-substrate interactions. Tunneling  $I(V)$  spectra show the dot/Ge(001) contact to exhibit marked current rectifying behavior, which is extremely well confined to the contact area. © 2006 American Institute of Physics.  
[DOI: 10.1063/1.2201861]

Fabrication of ordered, size selected, nanoscale wires and dots is an area of great interest. Due to their low dimensionality, they can exhibit quantum effects and may find use in future electronic and high density storage devices. Many methods have been put forward for the growth of such structures including pulsing scanning tunneling microscopy (STM) probes,<sup>1</sup> deposition of preformed clusters from the liquid or gas phase,<sup>2</sup> and thermal evaporation onto nanopatterned substrates, e.g., surfaces with strain relief patterns.<sup>3,4</sup> Substrates with well defined surface reconstructions have also been studied, such as the deposition of alkali metals onto the  $(7 \times 7)$  reconstructed Si(111) surface, to form so-called (2D) “magic” dots.<sup>5,6</sup> Dot arrays of magnetic materials are of added interest, offering the possibility of extremely high density magnetic data storage.<sup>7-10</sup>

In this letter we present the growth of ordered, uniformly sized, 2D Fe dots on the  $(2 \times 1)$  reconstructed Ge(001) surface and demonstrate current rectifying properties of the contact, using scanning tunneling spectroscopy (STS). Experiments were performed in a UHV system with a base pressure of  $1 \times 10^{-10}$  Torr. Samples were cut from a 2 in., Sb-doped ( $0.05 \text{ \Omega cm}$ ), Ge wafer. Fe was evaporated from an ultrapure rod, using an e-beam evaporator. Depositions were performed at room temperature. Nominal film thickness was measured using a quartz crystal balance. Auger electron spectroscopy (AES) was employed routinely to ensure surface cleanliness. STM was performed, at room temperature, using a home built instrument with an Omicron SCALA controller.

Ge(001) samples were outgassed at 800 K for 24 h in UHV. The surface was then subjected to repeated cycles of  $\text{Ar}^+$  ion etching and UHV annealing, at temperatures in the 850–950 K range.<sup>11,12</sup> AES shows a contaminant-free surface and the well known  $(2 \times 1)$  low energy electron diffraction (LEED) mesh is observed [Fig. 1(a)]. STM images large terraces with Ge dimer rows oriented along the  $[1\bar{1}0]$  direction, in agreement with earlier studies.<sup>11,12</sup> The dimer row direction rotates by  $90^\circ$  from one terrace to the next. The dimer formation results in the  $(2 \times 1)$  reconstruction, with a  $4 \text{ \AA}$  periodicity along the dimer rows and an  $8 \text{ \AA}$  periodicity across, as shown schematically in Fig. 1(b). At room temperature the Ge dimers flip-flop randomly between the two

equivalent positions.<sup>13</sup> In the locality of surface defects the flip-flop motion freezes, resulting in local areas of  $c(4 \times 2)$  reconstruction.<sup>14</sup> STS measured a band gap  $\sim 0.75 \text{ eV}$ , again consistent with previous studies.<sup>11</sup>

Submonolayer Fe films were deposited onto the clean surface, at a rate  $\sim 0.5 \text{ ML/min}$ . STM images showing the initial stages of growth are presented in Fig. 2. Fe surface coverage corresponds to  $\sim 8\%$ . The surface is characterized by the formation of nanoscale Fe dots. The substrate maintains its dimer row structure; however, the  $(2 \times 1)$  reconstruction that occurs over long ranges for the clean surface breaks down somewhat following film deposition. It is apparent that localized freezing of Ge dimers occurs, resulting in this loss of  $(2 \times 1)$  order. Despite the expectation of a reactive interface, the images suggest that the Fe dots form an abrupt interface, with no evidence for intermixing, such as surface voids,<sup>10</sup> imaged. This agrees with recent work showing low intermixing for this system, at room temperature.<sup>15</sup> In the direction perpendicular to the Ge dimer rows, virtually all dots have a full width at half maximum (FWHM)  $\sim 12 \text{ \AA}$ . Along the dimer rows they have an  $\sim 8 \text{ \AA}$  FWHM. They are thus visibly elongated across the dimer rows. This point is further evident from the fact that, like the dimer rows themselves, the dots can be seen to rotate by  $90^\circ$  from one terrace to the next [Fig. 2(b)]. For tunneling set points of  $I_t \sim 0.1 \text{ nA}$ , and  $V_b$  in the  $+0.7$  to  $+2 \text{ V}$  range, the dots have highly reproducible corrugation heights of  $1.1 \pm 0.1 \text{ \AA}$ , with respect to the underlying substrate. This shows them to be a single Fe monolayer in height. These  $1.1 \text{ \AA}$  high dots with lateral dimensions  $\sim 12 \times 8 \text{ \AA}^2$  predominate. Assuming pseudomorphic growth, and no intermixing, the observed di-

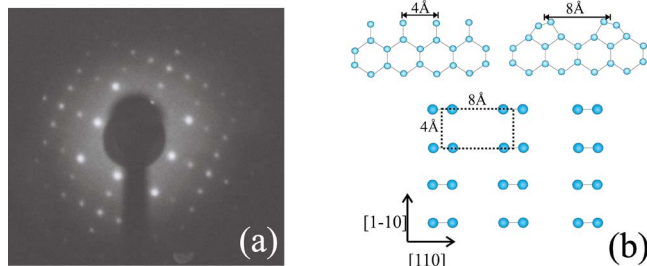


FIG. 1. (Color online) (a) LEED mesh of clean Ge(001) surface. (b) Model of accepted termination of Ge(001) surface. Top left: side view of unreconstructed surface. Top right: the energy lowering dimer formation that gives the  $(2 \times 1)$  symmetry. The two dimers shown are buckled in either equivalent position. Bottom: top down view of the  $(2 \times 1)$  surface.

<sup>a)</sup> Author to whom correspondence should be addressed; electronic mail: jordank@tcd.ie

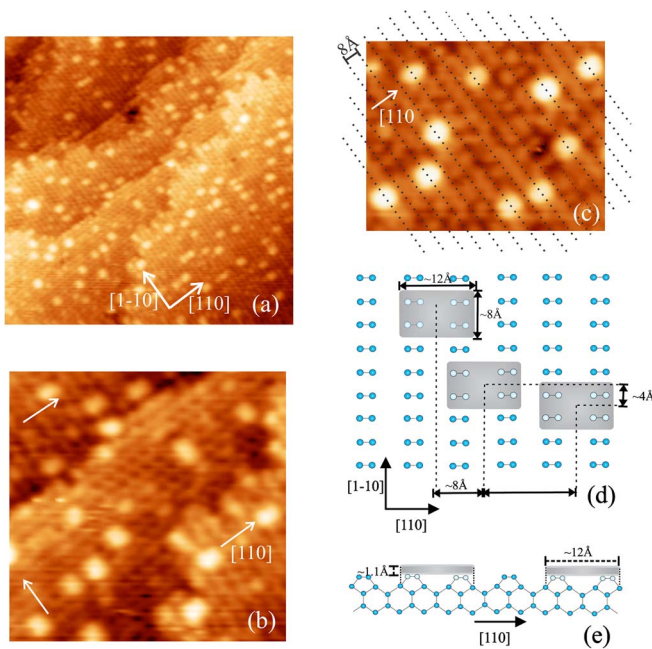


FIG. 2. (Color online) (a)  $370 \times 370 \text{ \AA}^2$  empty state STM image of Ge(001) surface following deposition of  $\sim 0.08$  ML Fe. (b)  $135 \times 135 \text{ \AA}^2$  STM zoom in, showing the dots, elongated across the dimer rows, rotate from one terrace to the next. (c)  $110 \times 90 \text{ \AA}^2$  STM image. The dashed lines along  $[1\bar{1}0]$  are separated by  $8 \text{ \AA}$ . These lines always pass through the center of the dots, illustrating the definite registry of the dots with the substrate. The loss of long range  $(2 \times 1)$  symmetry, characteristic of clean Ge(001), is also evident from this image. (d) Model of registry of the Fe dots on the  $(2 \times 1)$  Ge(001) surface. As a result of the observed spacing, it can be concluded that all dots nucleate at equivalent positions, as shown here. (e) Side view of dots with respect to the surface.

mensions are consistent with dots composed of  $\sim 10\text{--}12$  Fe atoms. Variant structures, mainly  $6 \times 8$ ,  $18 \times 8$ , and  $24 \times 8 \text{ \AA}^2$  dots, exist but account for  $\ll 5\%$  of imaged dots.

As the substrate maintains the dimer row structure the exact registry of the dots, with respect to the substrate, can be ascertained. In Fig. 2(c) dashed lines, along the  $[1\bar{1}0]$  oriented dimer rows, are separated by  $8 \text{ \AA}$ . It can be seen that these dashed lines pass through local depressions on the substrate surface. As the sample is positively biased these de-

pressions correspond to the electron rich buckled up atoms of frozen Ge dimers.<sup>13</sup> The lines always pass through the center of Fe dots, showing that dots nucleate exclusively on sites that are  $8 \text{ \AA}$  apart, or whole multiples thereof, in the  $[110]$  direction. Similarly, along the  $[1\bar{1}0]$  direction, the dots nucleate on sites separated by  $4 \text{ \AA}$ , or whole multiples thereof. All dots nucleate at the equivalent surface site outlined in the schematic of Fig. 2(d). Considering this registry, the observed  $8 \text{ \AA}$  FWHM along  $[1\bar{1}0]$  is easily explained in terms of nucleation across two dimer rows, as shown in Fig. 2(d). However, the  $12 \text{ \AA}$  FWHM in the  $[110]$  direction does not map out the  $8 \text{ \AA}$  periodicity of the Ge dimer rows in this direction, instead the observed width appears to be dictated by the  $4 \text{ \AA}$  periodicity of the subsurface Ge layer, as shown schematically in Fig. 2(e). This is an indication that the Fe dots do not interact solely with the reconstructed Ge dimers of the surface, but also with the subsurface Ge layer. This, along with the imaged localized freezing of the flip-flopping surface dimers, suggests a strong dot-substrate interaction.

The observed size uniformity of the dots points to the existence of a local energy minimum. There are, in our view, two possible explanations for the existence of this minimum; a magic number effect or adsorbate-substrate interactions. An interplay of these two processes is also a possibility. It is known that energy minima can exist for isolated clusters, of a certain magic size, in free space, due to the electronic shell effect of quantum confined electrons.<sup>16</sup> This mechanism was recently used to explain the nucleation of Co nanodots on a  $\text{Si}_3\text{N}_4$  buffer layer.<sup>7</sup> This mechanism cannot be ruled out for the system studied here; however, as a clear dot-substrate interaction is present one would expect quantum confinement effects to be inhibited. Also, the existence of some variant cluster sizes suggests that sizes other than the dominant ones are energetically unfavorable, as opposed to forbidden by a magic rule.

The second explanation for the uniform dot size is the existence of an energy minimum due to adsorbate-substrate interactions. Such interactions can explain the dot size [lateral dimensions corresponding to exactly  $(3 \times 2)$  the Ge(001) unreconstructed surface unit cell], and interdot spac-

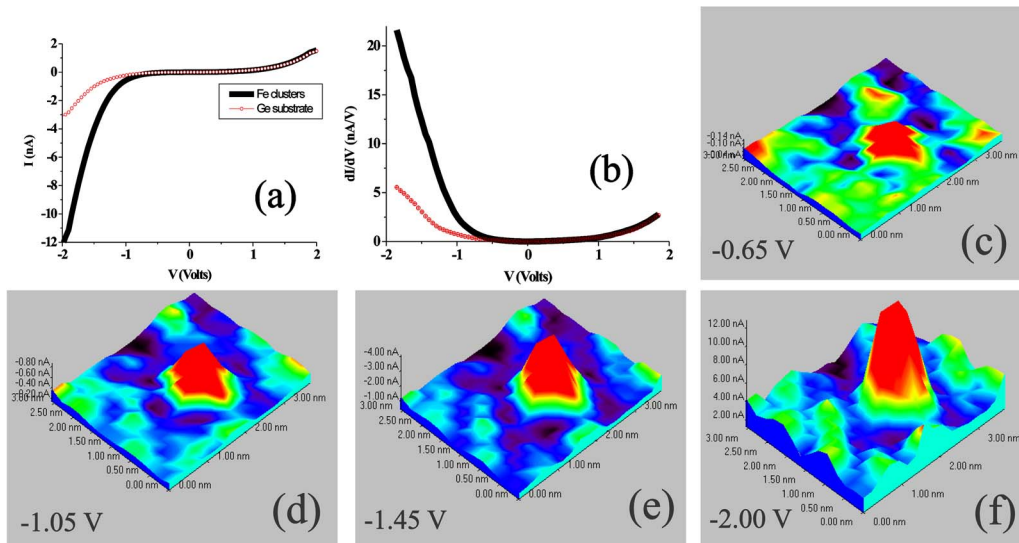


FIG. 3. (Color online) (a)  $I(V)$  tunneling spectra over Fe dots (thick solid) and surrounding Ge(001) substrate (thin circles). Marked current rectification due to the dots is evident. (b) Derivative of  $I(V)$  spectra. Dots have band gap  $\sim 0.65 \text{ V}$ , and surrounding substrate  $\sim 0.75 \text{ V}$ . [(c)–(f)]  $I(V)$  map obtained over a single Fe dot. Current rectification is well confined to area over the dot. No change in tunneling behavior of surrounding substrate observed.



ing, which maps out the periodicity of the substrate. Indeed, at a more basic level, the edges of the rectangular shaped dots are oriented along the principle axes of the substrate, clearly illustrating the influence of the surface symmetry on dot nucleation. In this respect, the observed Fe dot nucleation is similar to that for 2D arrays grown on surfaces with a periodic strain relief pattern.<sup>3,4</sup> While an exact stabilization mechanism is not easily identified, it would appear that a local potential well is formed at the observed nucleation site. One possible mechanism is that an adsorbed Fe atom (or cluster of atoms) can induce an extremely localized  $c(4 \times 2)$  reconstructed surface unit cell. The center of this reconstructed unit cell could then act as a potential well, trapping newly arriving Fe atoms, until the stable dot size is reached. Low mobility, due to the existence of a single nucleation site, appears instrumental in making the merging of dots unfavorable, as dots would have to jump to equivalent sites to diffuse across the surface.

Further to assembly of low dimensional structures, the demonstration of useful functions is also of great importance, as it illustrates potential for use in future devices. Figures 3(a) and 3(b) present tunneling  $I(V)$  spectra, and their derivative, for the Fe dots and surrounding Ge(001) surface. Each curve is the average of  $\sim 300$  individual curves. The Ge(001) surface exhibits a band gap unchanged from that of the clean surface,  $\sim 0.75$  eV. The Fe dots are semiconducting, with a band gap  $\sim 0.65$  eV. Spectra obtained above the dots exhibit marked current rectifying behavior. The junction is in forward bias for negative sample voltage, as expected for tunneling through a Schottky contact on an  $n$ -type semiconductor. The threshold voltage is  $\sim -0.85 \pm 0.2$  V.

A representative  $I(V)$  map obtained in the area of an Fe dot is presented in Figs. 3(c)–3(f). The complete spatial confinement of the rectifying properties to the area of the dot is immediately evident. Such confinement shows that it is possible to fabricate closely packed discrete nanoscale rectifying junctions, which could yield a data density value of four orders of magnitude higher than currently available. Considering the measured dot size and surface coverage ( $\sim 8\%$ ), a dot density value  $\sim 6.25 \times 10^{16}$  dots/m<sup>2</sup>, or  $4 \times 10^4$  Gdot/in.<sup>2</sup>, is calculated for the surface imaged here.

The map also illustrates other properties brought about due to the nanoscale size of the contact. Metal induced gap states (MIGSs) have conclusively been shown to exist in the semiconductor substrate for large scale metal-semiconductor contacts.<sup>17</sup> However, no MIGSs are resolved here, a consequence of the absence of metallic states for the Fe dots. Similarly,  $I(V)$  maps, over the area of the Fe dots, for volt-

ages within the band gap region of the substrate (not shown), suggest that no interface states or defect states are present. The absence of such states can be attributed to the excellent interface quality, which can be seen to be atomically abrupt, again made possible due to the size of the contact. We note that as MIGSs do not exist, and the interface is near ideal, these nanoscale contacts differ from conventional Schottky contacts. Indeed, it is possible that, due to the absence of states in the band gap that are responsible for Fermi level pinning, nanoscale contacts could allow tailored Schottky barrier heights simply through the use of elements of different work functions to form the dots.

In conclusion, the  $(2 \times 1)$  reconstructed surface of Ge(001) represents a suitable template for growth of well ordered, uniformly sized, 2D Fe dots. All dots nucleate at an equivalent surface site. Their size, shape, and the observed interdot spacing are dictated by the substrate. The  $I(V)$  characteristics of the dots show highly reproducible and spatially confined Schottky contacts are formed towards the lowest size limit of the metal-semiconductor interface.

Financial support from Science Foundation Ireland, Contract No. 00/PI.1/C042, is gratefully acknowledged.

<sup>1</sup>D. Fujita and T. Kumakura, Appl. Phys. Lett. **82**, 2329 (2003).

<sup>2</sup>B. Kaiser and B. Stegemann, ChemPhysChem **5**, 37 (2004).

<sup>3</sup>H. Brune, M. Giovannini, K. Bromann, and K. Kern, Nature (London) **394**, 451 (1998).

<sup>4</sup>H. Y. Lin, Y. P. Chiu, L. W. Huang, Y. W. Chen, T. Y. Fu, C. S. Chang, and T. T. Tsong, Phys. Rev. Lett. **94**, 136101 (2005).

<sup>5</sup>M. Y. Lai and Y. L. Wang, Phys. Rev. Lett. **81**, 164 (1998).

<sup>6</sup>Jian-Long Li, Jin-Feng Jia, Xue-Jin Liang, Xi Liu, Jun-Zhong Wang, Qi-Kun Xue, Zhi-Qiang Li, John S. Tse, Zhenyu Zhang, and S. B. Zhang, Phys. Rev. Lett. **88**, 066101 (2002).

<sup>7</sup>Shangir Gwo, Chung-Pin Chou, Chung-Lin Wu, Yi-Jen Ye, Shu-Ju Tsai, Wen-Chin Lin, and Minn-Tsong Lin, Phys. Rev. Lett. **90**, 185506 (2003).

<sup>8</sup>J. M. Gallego, S. Yu Grachev, M. C. G. Passeggi, Jr., F. Sacharowitz, D. Ecija, R. Miranda, and D. O. Boerma, Phys. Rev. B **69**, 121404 (2004).

<sup>9</sup>Yoshiaki Nakamura, Yasushi Nagadomi, Sung-Pyo Cho, Nobuo Tanaka, and Masakazu Ichikawa, Phys. Rev. B **72**, 075404 (2005).

<sup>10</sup>M. A. K. Zilani, Y. Y. Sun, H. Xu, Lei Liu, Y. P. Feng, X.-S. Wang, and A. T. S. Wee, Phys. Rev. B **72**, 193402 (2005).

<sup>11</sup>J. A. Kubby, J. E. Griffith, R. S. Becker, and J. S. Vickers, Phys. Rev. B **36**, 6079 (1987).

<sup>12</sup>H. J. W. Zandvliet, Phys. Rep. **388**, 1 (2003).

<sup>13</sup>D. J. Chadi, Phys. Rev. Lett. **43**, 43 (1979).

<sup>14</sup>W. S. Yang, X. D. Wang, K. Cho, J. Kishimoto, S. Fukatsu, T. Hashizume, and T. Sakurai, Phys. Rev. B **50**, 2406 (1994).

<sup>15</sup>M. Cantoni, M. Riva, G. Isella, R. Bertacco, and F. Ciccacci, J. Appl. Phys. **97**, 093906 (2005).

<sup>16</sup>W. D. Knight, K. Clemenger, W. A. de Heer, W. A. Saunders, M. Y. Chou, and M. L. Cohen, Phys. Rev. Lett. **52**, 2141 (1984).

<sup>17</sup>T. C. G. Reusch, M. Wenderoth, L. Winking, N. Quass, and R. G. Ulbrich, Appl. Phys. Lett. **87**, 093103 (2005).